Correlation Between Structural and Functional Connectivity Impairment in Amyotrophic Lateral Sclerosis

Ruben Schmidt,[1]* Esther Verstraete,[1] Marcel A. de Reus,[2] Jan H. Veldink,[1] Leonard H. van den Berg,[1] and Martijn P. van den Heuvel[2]

[1]*Department of Neurology, Brain Center Rudolf Magnus, University Medical Center Utrecht, Utrecht, Netherlands*
[2]*Department of Psychiatry, Brain Center Rudolf Magnus, University Medical Center Utrecht, Utrecht, Netherlands*

Abstract: Amyotrophic lateral sclerosis (ALS) is a fatal neurodegenerative disease, characterized by progressive loss of motor function. While the pathogenesis of ALS remains largely unknown, imaging studies of the brain should lead to more insight into structural and functional disease effects on the brain network, which may provide valuable information on the underlying disease process. This study investigates the correlation between changes in structural connectivity (SC) and functional connectivity (FC) of the brain network in ALS. Structural reconstructions of the brain network, derived from diffusion weighted imaging (DWI), were obtained from 64 patients and 27 healthy controls. Functional interactions between brain regions were derived from resting-state fMRI. Our results show that (i) the most structurally affected connections considerably overlap with the most functionally impaired connections, (ii) direct connections of the motor cortex are both structurally and functionally more affected than connections at greater topological distance from the motor cortex, and (iii) there is a strong positive correlation between changes in SC and FC averaged per brain region ($r = 0.44$, $P < 0.0001$). Our findings indicate that structural and functional network degeneration in ALS is coupled, suggesting the pathogenic process affects both SC and FC of the brain, with the most prominent effects in SC. *Hum Brain Mapp 35:4386–4395, 2014.* © 2014 The Authors. Human Brain Mapping Published by Wiley Periodicals, Inc.

Key words: amyotrophic lateral sclerosis; magnetic resonance imaging; diffusion weighted imaging; resting-state; connectivity

---

INTRODUCTION

Amyotrophic lateral sclerosis (ALS) is a severe neurodegenerative disease characterized by progressive degeneration of both upper and lower motor neurons. With a median survival of 3 years after onset of symptoms [del Aguila et al., 2003; Hardiman et al., 2011], patients experience deteriorating motor function and eventually fatal respiratory failure. While a multitude of structural and functional imaging studies have reported disease effects in the brain, only a few have directly related structural to functional effects. No consensus has been reached yet on the interplay between structural and functional changes

TABLE I. Subject demographics and clinical characteristics

	Healthy control subjects (*n* = 27) Mean ± SD (range)	Patients (*n* = 64) Mean ± SD (range)	
Age (years)	57.7 ± 11.6 (35–78)	56.9 ± 12.0 (24–79)	
Male/Female	19/8	48/16	
Site of onset [*n* (%)]		Bulbar	9 (14)
		Cervical	35 (55)
		Thoracic	0 (0)
		Lumbosacral	17 (27)
		Spinal	3 (5)
Diagnostic category [*n* (%)]		Definite ALS	8 (13)
		Probable ALS	32 (50)
		Probable ALS Lab Supported	17 (27)
		Possible ALS	7 (11)
Disease duration at scan date (months)		16.5 ± 8.0 (4–103)	
ALSFRS-R		40 ± 3.5 (30–47)	
Progression rate		0.64 ± 0.43 (0.06–1.70)	

SD, standard deviation; ALSFRS-R, revised ALS functional rating scale; Progression rate, (48–ALSFRS-R)/(disease duration in months).

observed in ALS. A better understanding of the coupling between structural and functional disease effects in the brain on a macroscopic level may provide tools to extend our knowledge of the underlying disease process. In addition, for future application of imaging markers in the diagnostic phase or to monitor disease evolution it is of relevance to know how these measures relate to each other.

The brain is an integrative complex system, rather than a collection of independently operating regions [Sporns, 2006; Stam and Reijneveld, 2007; van den Heuvel and Hulshoff Pol, 2010]. Hence, disease effects of neuropsychiatric and neurological disorders can be found in altered brain connectivity [Seeley et al., 2009; Zalesky et al., 2010]. Although structural connectivity (SC) has been shown to underlie, to some extent, functional communication between segregated brain regions [Collin et al., 2013; Hagmann et al., 2008; van den Heuvel et al., 2013], our understanding of the relationship between changes in SC and functional connectivity (FC) in ALS remains sparse. Structural impairment of white matter tracts belonging to the motor system has been consistently found [Prudlo et al., 2012; Rose et al., 2012; Verstraete et al., 2010]. Previous findings of FC abnormalities, also mostly related to the motor system, however, are inconsistent. Reports of enhanced sensorimotor network connectivity [Agosta et al., 2011; Douaud et al., 2011], reduced premotor FC [Mohammadi et al., 2009] or a combination of increased and decreased FC [Zhou et al., 2013], leave the relation between changes in SC and FC an open question.

In the present study, both SC and FC changes were assessed based on diffusion weighted imaging (DWI) and resting-state functional MRI (rs-fMRI). Combining SC and FC in a cross-modal design, this study aims to elucidate the relation between SC and FC abnormalities in ALS patients from a network perspective, thereby providing more insight into how the pathogenic process affects the brain network.

MATERIALS AND METHODS

Patients

Sixty-four patients with sporadic or familial ALS (m/f: 48/16; mean age/SD: 56.9/12.0 years) and 27 healthy controls (m/f: 19/8; mean age/SD: 57.7/11.6 years) participated in this combined structural and FC study (see Table I for full demographics and clinical characteristics). Patients diagnosed with ALS according to the El Escorial criteria [Brooks et al., 2000] were recruited from the outpatient clinic for motor neuron diseases of the University Medical Center Utrecht. Subjects did not have a history of brain injury, epilepsy, psychiatric illness, or neurodegenerative diseases other than ALS. The Ethical Committee for research into humans of the University Medical Center Utrecht approved study protocols. All subjects provided informed written consent according to the Declaration of Helsinki.

Image Acquisition and Preprocessing

Imaging consisted of an anatomical T1-weighted image, DWI and rs-fMRI. All imaging data were acquired on a 3 Tesla Philips Achieva Medical Scanner with a SENSE receiver head-coil. A high-resolution T1-weighted image was acquired for anatomical reference using the following parameters: 3D FFE using parallel imaging; TR/TE = 10/4.6 ms, flip-angle 8°, slice orientation: sagittal, $0.75 \times 0.75 \times 0.8$ mm voxelsize, FOV = $160 \times 240 \times 240$ mm, reconstruction matrix = $200 \times 320 \times 320$ covering the whole brain.

Cortical and subcortical brain regions were selected by parcellating the cerebrum and the brain stem into distinct, anatomically separated brain regions on the basis of the T1-weighted image, using the well-validated Freesurfer suite (V4.5, http://surfer.nmr.mgh.harvard.edu/). This included the automatic segmentation of gray and white matter tissue, followed by parcellation of the segmented gray matter mask into distinct brain regions, based on a normalized template, parcellating the brain into a number of brain regions, including left and right caudate nucleus, globus pallidum, nucleus accumbens, thalamus, amygdala, hippocampus, brain stem, and 68 cortical brain regions. In total, 83 distinct brain regions were parcellated [Fischl et al., 1999, 2004].

DWI was performed to reconstruct the white matter tracts collectively forming the structural brain network. From all subjects 2 sets of 30 weighted diffusion scans and 5 unweighted B0 scans each, were acquired as follows: DWI-MR using parallel imaging SENSE p-reduction 3; high angular gradient set of 30 different weighted directions, TR/TE = 7035/68 ms, $2 \times 2 \times 2$ mm voxel size, 75 slices, $b = 1000$ s/mm^2, second set with reversed k-space read-out.

DWI preprocessing included corrections for susceptibility and eddy-current distortions, as was previously described by Verstraete et al. [2011]. The diffusion profile in each voxel of the resulting image was fitted a tensor, using a robust fit method based on M-estimators [Chang et al., 2005]. From the fitted tensors, the fractional anisotropy (FA) and preferred diffusion direction, corresponding to the tensor's principal eigenvector, were derived for each voxel.

White matter tracts were reconstructed using Fiber Assignment by Continuous Tracking (FACT) [Mori and van Zijl, 2002; Mori et al., 1999, 2002]. In each white voxel of the brain mask white matter fibers were tracked, initiated by 8 seeds, going from voxel to voxel following the main diffusion direction in each traversed voxel. Stopping conditions for fiber tracking were: a voxel was reached with an FA value lower than 0.1, the trajectory of the trace fiber exceeded the brain mask or the streamline made a turn of more than 45°. Furthermore, only streamlines longer than 30 mm were considered for analysis.

Brain networks were mathematically described as graphs. A graph consists of a collection of nodes and a collection of connections linking these nodes. Here, the nodes were taken as the 83 segmented brain regions and the connections represented the white matter pathways interlinking the regions. For each dataset of both patients and healthy controls, an individual brain network was reconstructed [van den Heuvel and Sporns, 2011; Verstraete et al., 2011]. Individual brain networks were reconstructed as follows: first, from the total collection of reconstructed streamlines, those that touched both region i and region j were selected. Then, from the selected fiber streamlines, the average FA values were computed as the average over all points and all included streamlines. This value was incorporated into cell $c(i,j)$ in the SC matrix. If no tracts were found between regions i and j, the corresponding cell of the SC matrix was assigned a value of zero, reflecting the nonexistence of a direct tract between regions i and j in the brain network. To avoid potential spurious fibers, connections were considered to be present if made up of more than one streamline. This procedure was repeated for all regions that make up the collection of nodes to obtain an undirected, weighted graph describing the brain network's structure.

Resting-state blood oxygen level-dependent (BOLD) signals were recorded for a duration of 8 min. Acquisition parameters: 3D PRESTOSENSE p/s-reduction 2/2, TR/TE = 22/32 ms using shifted echo, slice orientation: sagittal, flip-angle 10°, dynamic scan time 0.5 s, voxel-size $4 \times 4 \times 3.9$ mm, FOV = $160 \times 256 \times 224$ mm, reconstruction matrix = $40 \times 64 \times 57$ (covering whole brain). A short volume acquisition was used to allow for a comprehensive sample mitigating aliasing of biorhythms in the frequency domain up to 1 Hz, effectively minimizing the contribution of respiratory and cardiac oscillations (0.3 and >0.8 Hz, respectively) into the resting-state lower frequencies of interest (0.01–0.1 Hz) [Cordes et al., 2001]. Preprocessing of the rs-fMRI data was performed with the SPM8 software package (http://www.fil.ion.ucl.ac.uk) and consisted of four steps. First, correcting for possible small head movements, functional time-series were realigned. Second, to ensure overlap with the cortical parcellation maps, the timeseries were coregistered with the T1-weighted image. Third, global mean signal, signal of ventricles, the average time-series of white matter voxels, and six motion parameters (resulting from the realignment process) were regressed out of the timeseries of each voxel to minimize effects of global signal drifts and potential movement. Fourth and last, resting-state timeseries were bandpass filtered to select the resting-state frequencies of interest (0.01–0.08 Hz).

FC between brain regions was assessed on the basis of correlation analysis. A mean resting-state fMRI time-series was obtained by averaging over the time-series of all voxels contained in brain region i. Likewise, a mean resting-state fMRI time-series was obtained for region j. The Pearson correlation coefficient between these mean timeseries, indicating the level of FC between region i and j, was entered into cell $c(i,j)$ of the FC matrix. Negative correlation coefficients, reflecting functionally distinct brain regions [Chai et al., 2012; Fox et al., 2005], were set to zero to mark these brain regions as unconnected. An undirected, weighted graph describing the brain network's functional layout was obtained by computing correlations between all 83 brain regions.

Statistical Analyses

Statistical analyses of altered SC and FC were carried out on the basis of structural and functional group matrices, containing the means of corresponding nonzero entries in individual matrices of all members of the group, i.e. patients or healthy controls. Direct connections were obtained by requiring connections to be defined in both the SC and the FC matrix. A mask was created to ensure
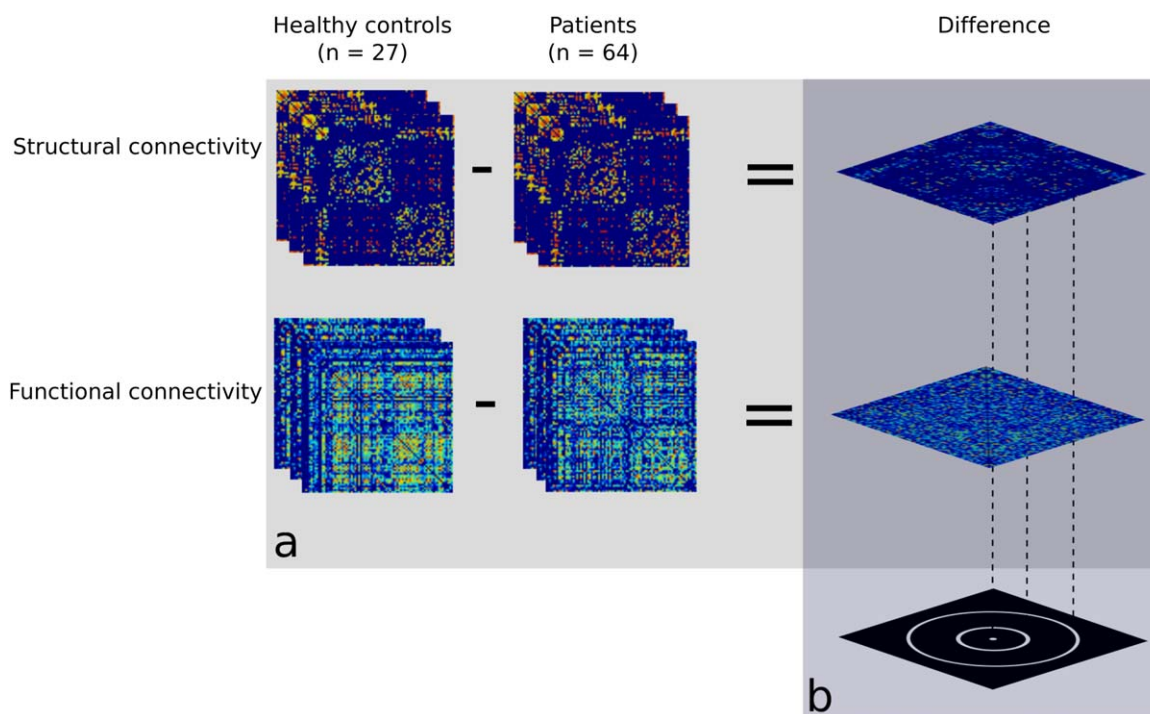
Figure 1.

(**a**) Determination of changes in structural and functional connectivity in patients compared with healthy controls using difference matrices, i.e., the difference between the average connectivity matrix in healthy controls and the average connectivity matrix in patients. (**b**) Selection of connections between rings of nodes surrounding the motor cortex. [Color figure can be viewed in the online issue, which is available at wileyonlinelibrary.com.]

the same set of connections was compared between patients and healthy control subjects. The group mask was constructed using intersection criteria: connections had to be present in at least 50% of the patients and, as an additional requirement the connections had to be present in a minimum of 50% of the control subjects. A total of 460 connections remained for analysis, corresponding to a sparsity of 13.5% (460/(83*82/2)).

Overlap Between Changes in Structural and Functional Connectivity

Affected structural and functional connections were examined using the definition of a difference matrix. The difference matrices for SC and FC were obtained by subtracting the patients' group matrix from the healthy controls' group matrix (Fig. 1a). The connections were ordered by their impairment to select the most impaired structural and functional connections. Between these structural and functional connections, the overlap was determined as the number of overlapping elements, tested for statistical significance against the distribution of overlaps based on 10,000 runs of two random selections. Overlaps were determined for selections ranging from the top 1% to the top 30% most impaired

connections. The upper bound was chosen to be 30% to ensure the selected connections were clearly impaired.

Changes in Connectivity as a Function of Topological Distance from the Motor Cortex

The motor cortex is known to play a central role in the affected structural brain network in ALS patients. To compare its involvement in FC to its role in SC, the nodes surrounding the left and right motor cortex (defined as the precentral gyrus and the paracentral lobule) were assigned a ring according to their topological distance (i.e., smallest number of steps) from the motor cortex in the healthy controls' structural group matrix. In both hemispheres (including the brain stem), two rings of nodes surrounding the motor cortex were thus defined. Accordingly, two sets of connections were distinguished: connections between the motor cortex and the first ring nodes (first ring connections) and connections between the first and second ring nodes (second ring connections). For the first and second ring connections the differences in SC and FC were extracted from the difference matrices, as illustrated by Figure 1b. The average changes in SC and FC of first and second ring connections reflect the SC and FC impairment
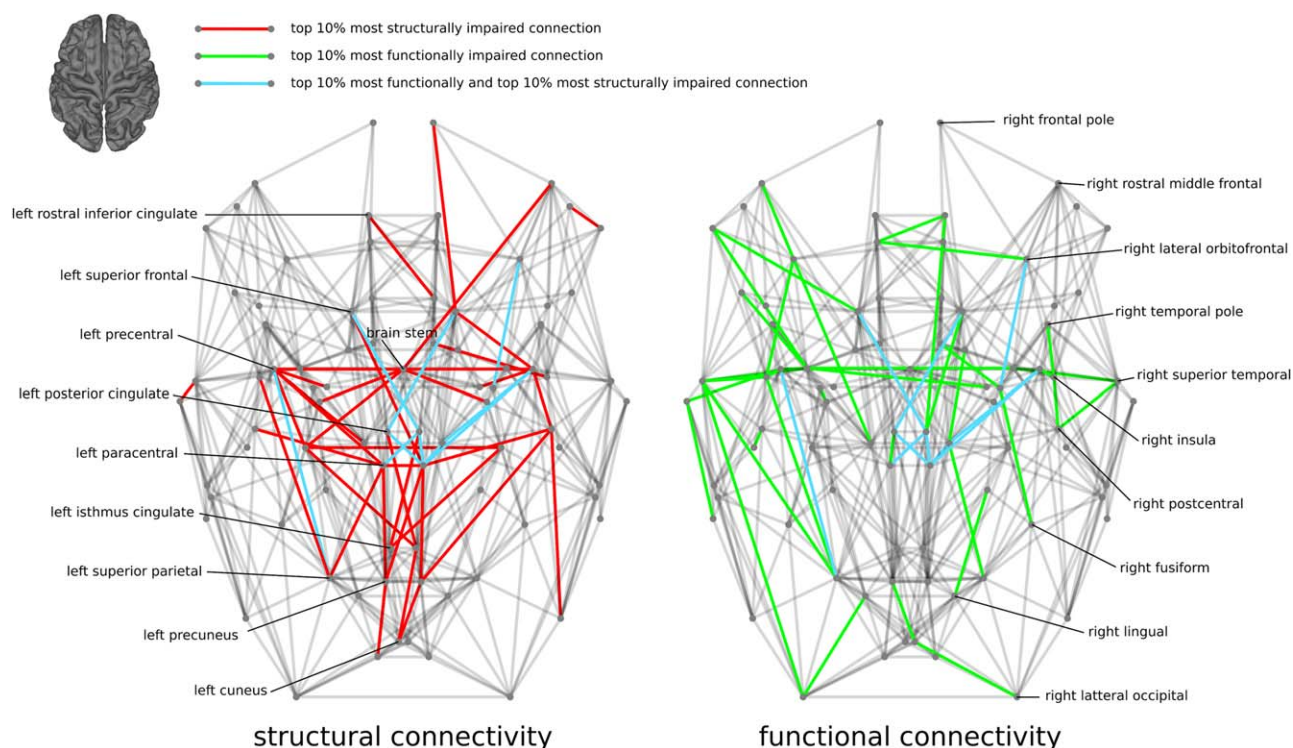
Figure 2.

Connectomic representation of the brain network in which the top 10% most impaired SC connections (left) and the top 10% most impaired FC connections (right) as well as the overlapping connections are colored. The locations of homologous nodes, based on anatomy, have been symmetrized. [Color figure can be viewed in the online issue, which is available at wileyonlinelibrary.com.]

profile as a function of topological distance from the motor cortex. Group SC and FC changes found in first ring connections were compared to changes in the second ring connections using a two-sample *t*-test, to examine whether connectivity impairment differed in connections close to or distant from the motor cortex. Paired *t*-tests were carried out per ring on SC and FC between healthy controls and patients, to check whether the average connectivity differences were significant.

Correlation Between SC and FC Differences

The association between SC and FC differences was examined on the whole brain level, not bounded by the subnetwork surrounding the motor cortex as in the previous analysis, by investigating the correlation between differences in SC and FC based on all connections. The mean difference in SC and the mean difference in FC between patients and healthy controls were computed for each node's direct connections. The relationship between node-wise SC and FC differences was determined by means of correlation analysis.

RESULTS

Overlap Between Changes in Structural and Functional Connectivity

The observed overlap between the top 10% most impaired structural and functional connections, Figure 2, is significantly larger than expected for random connections ($P = 0.003$). Of the 46 top 10% most impaired connections, the 10 connections that overlapped, mainly involving the motor cortex, are tabulated in Table II. A significantly larger overlap is also seen in the top 20–30% most impaired structural and functional connections ($P < 0.03$). Figure 3 shows the overlaps between changes in SC and FC for selections ranging from the top 1% to the top 30%, along with the overlaps between two sets of randomly chosen connections.

Changes in Connectivity as a Function of Topological Distance from the Motor Cortex

Changes in SC and FC in first and second ring connections surrounding the right motor cortex are presented graphically in Figure 4. Figure 5 summarizes the effects in

TABLE II. Tabulation of overlapping connections among the 10% most impaired structural connections and the 10% most impaired functional connections

Overlapping connections

Left precentral	Left superior parietal
Left paracentral	Right posterior cingulate
Right precentral	Right paracentral
Right paracentral	Left posterior cingulate
Right precentral	Right thalamus proper
Right paracentral	Right thalamus proper
Right paracentral	Right posterior cingulate
Left superior frontal	Right posterior cingulate
Right superior frontal	Left posterior cingulate
Right lateral orbitofrontal	Right amygdala

SC and FC per ring. Results of the left hemisphere are similar and are displayed in Supporting Information Figures S1 and S2. On average, structural impairment of first ring connections amounts to a decrease in FA of 2.0×10^{-2} ($P = 2.9 \times 10^{-6}$) and in the second ring this decrease is less than half as large as in the first ring: 0.8×10^{-2} ($P = 1.8 \times 10^{-5}$). The average FC impairment observed in first ring connections is a reduction in BOLD correlation coefficient of 3.7×10^{-2} ($P = 5.5 \times 10^{-4}$), indicating there is less or less efficient functional communication of the motor cortex with its directly connected brain regions. The second ring connections were found to be functionally unaffected in patients ($P = 0.42$). Table III lists all nodes along with their ring classification. The first ring connections are affected significantly more than those belonging to the second ring, both structurally ($P = 3.7 \times 10^{-3}$) and functionally ($P = 1.8 \times 10^{-3}$), suggesting SC and FC impairment are not independent but linked to one another.

In addition, correlations between first ring SC and FC impairment and the clinical metrics ALSFRS-R score and progression rate were explored. Individual average first ring SC impairment of the right motor cortex was found to be negatively correlated with ALSFRS-R score ($r = -0.29$, $P = 0.02$), Figure 6. No significant correlations were found between ALSFRS-R scores and second ring SC or FC impairments, Figure S3 Supporting Information.

Correlation Between SC and FC Differences

The scatter plot of Figure 7 shows the connectivity changes averaged per node. A significant positive correlation was observed between differences in SC and FC of $r = 0.44$ ($P = 3.6 \times 10^{-5}$), indicating a significant association between disease-related changes in SC and FC in ALS. The paracentral and precentral gyri, forming the motor cortex, stand out as being the most structurally impaired and at the same time the most functionally impaired nodes.

The whole brain edge-wise correlation, comparing SC and FC differences of individual connections, was found to be less strong ($r = 0.14$, $P < 0.0001$), Figure S4a Supporting Information.

DISCUSSION

The main finding of this study integrating DWI and rs-fMRI data is the positive correlation between changes in SC and FC in ALS, indicating that differences in white matter integrity and effects of FC go hand in hand. Moreover, direct connections between the motor cortex and other brain regions show the largest structural and functional impairments in patients with ALS.

Analysis of SC-FC overlap revealed a significantly larger overlap than expected by chance between the strongest SC and FC impairments, suggesting that disease-related reductions in SC and FC are not independent, but are rather coupled, possibly sharing the same pathological origin. Examining the influence of the topological distance from the motor cortex on the SC and FC deteriorations showed that SC and FC impairments are significantly larger at shorter topological distance from the motor cortex. This is in keeping with previous SC studies that have consistently found a central role for the motor cortex in brain network impairment [Cirillo et al., 2012; Verstraete et al., 2011, 2013]. The association between SC and FC impairments is demonstrated most straightforwardly by the observed significant association between node-wise SC
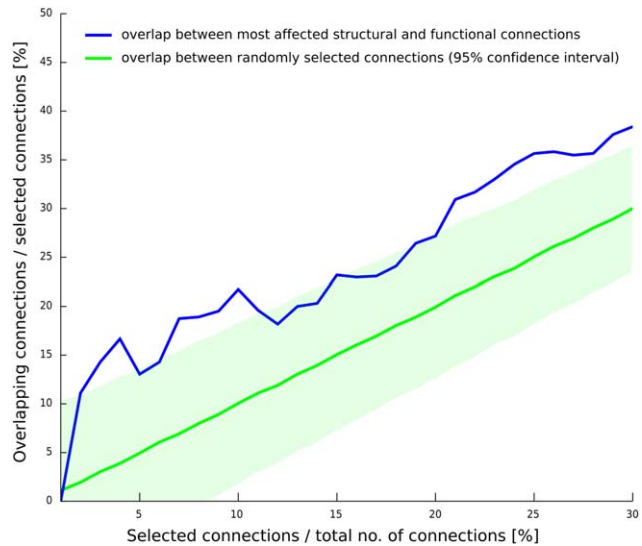

Figure 3.

Observed overlap between the most impaired structural and the most impaired functional connections in patients (blue). Overlaps were determined for selections (x-axis) ranging from the top 1% to the top 30%, corresponding to the most impaired 5–138 of a total of 460 connections. The average overlaps, along with 95% confidence intervals, found between randomly selected connections are displayed for comparison (green). The observed overlap for the top 10% most impaired structural and functional connections are higher than expected for random connections ($P = 0.003$). [Color figure can be viewed in the online issue, which is available at wileyonlinelibrary.com.]
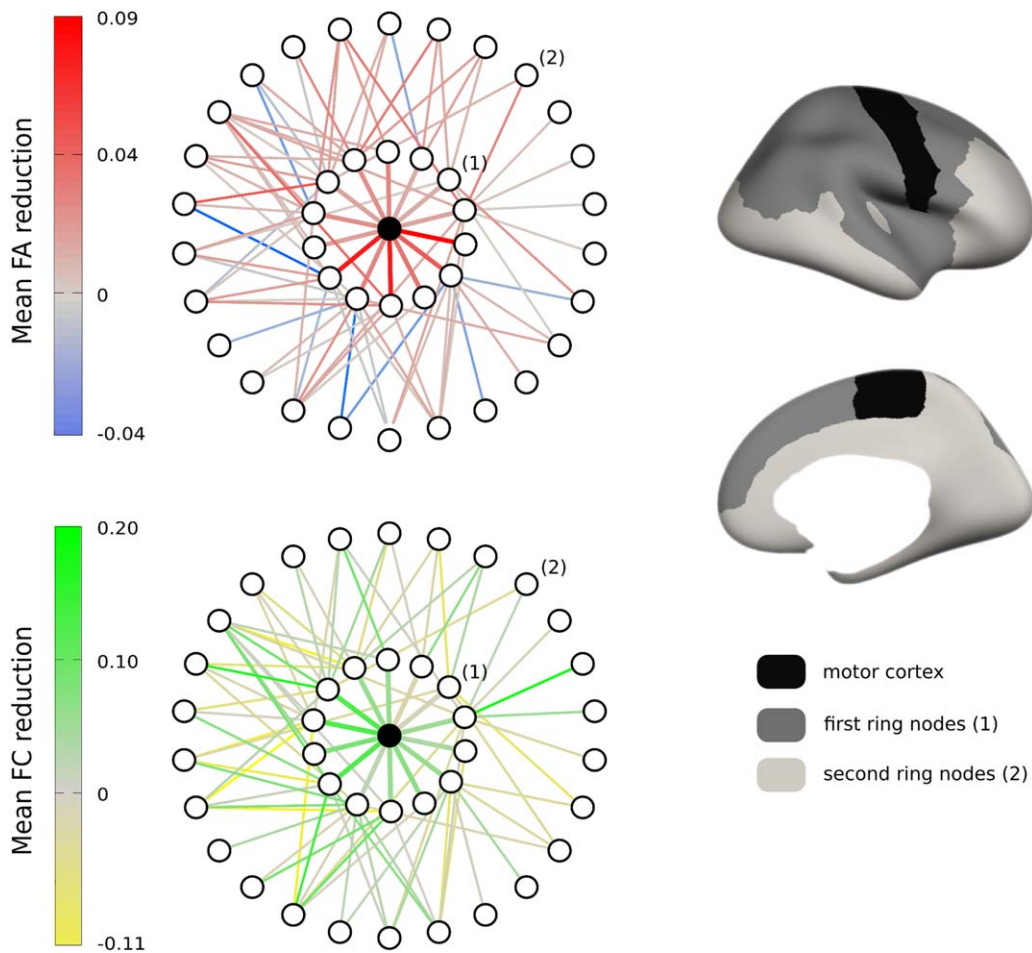
Figure 4.

Nodes connected to the right motor cortex are displayed in rings with a radius proportional to the topological distance from the right motor cortex. Connections in red or green correspond to structural or functional connections for which, respectively, reduced FA or FC was measured. (1) and (2) mark the first and second ring of nodes surrounding the motor cortex. The anatomical distribution of the cortical first and second ring nodes is shown in the medial and lateral brain images. First and second ring nodes are listed in Table III, starting from (1) and (2) going round clockwise. [Color figure can be viewed in the online issue, which is available at wileyonlinelibrary.com.]

and FC changes (Fig. 7). Among individual connections, no clear association between SC and FC impairments was observed, see Figure 2 and Supporting Information Figure S4a. Our findings for the first time show that on a connection level there is no clear linear relationship between the extent of structural and functional impairment, whereas in terms of brain regions SC and FC impairment do show linear coupling. Interestingly, a study modeling the impact of lesions in the human brain [Alstott et al., 2009], reported widespread changes in FC, especially for lesions along the cortical midline, while the effects of lesions in the primary sensory or motor regions remained more localized. Although more research is necessary to establish the link between structural and FC aberrations, these simulated effects are in support of our empirical findings of overlapping SC and FC impairments concentrated in the motor network (Table II).

Only a few other studies have directly investigated the relation between changes in structural and functional brain connectivity. Agosta et al. examined FA changes in the corticospinal tract (CST) as a measure for structural damage to the sensorimotor network (SMN) [Agosta et al., 2011], revealing that patients with CST damage showed the strongest reductions in FC, findings with which our results are in strong agreement. Douaud et al. correlated changes in SC with FC and, as opposed to our findings, reported enhanced FC for structurally impaired connections [Douaud et al., 2011]. In addition to FC impairments, our results also show significantly enhanced FC, most markedly in the direct connections of the left caudate nucleus (Fig. 7), but not in
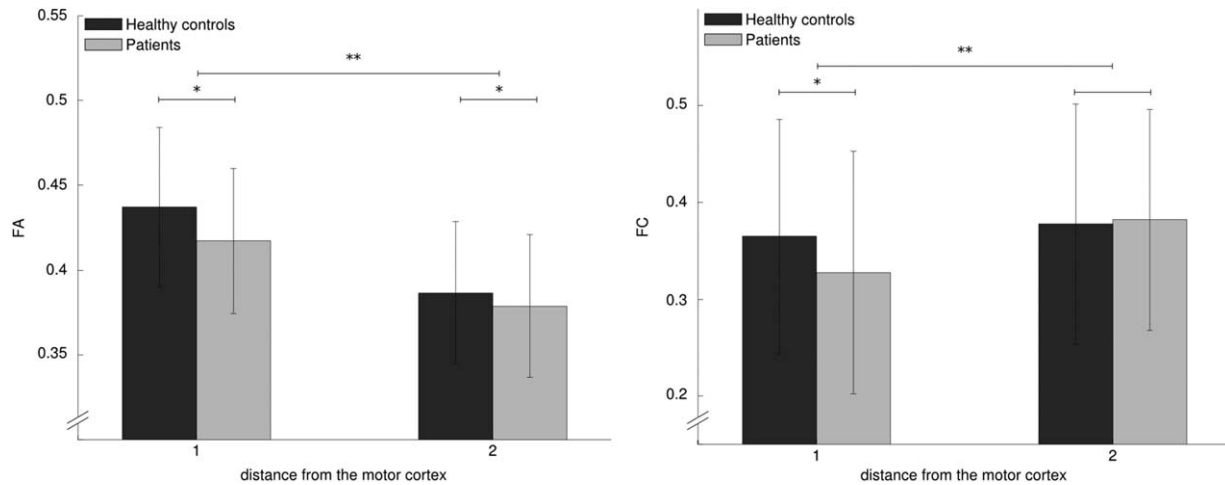
Figure 5.

FA and FC differences in patients at increasing topological distance from the right motor cortex. (*) Denotes significant differences between healthy controls and patients, (**) indicates impairment of the first and second ring differ significantly.

structurally affected brain regions. Future research should investigate the biological underpinnings for observed enhancements as well as impairments of FC in ALS.

The observed correlation between changes in SC and FC in ALS patients indicates that structural and functional effects are not independent, suggestive of a common underlying mechanism. The functionally unaffected, but structurally impaired second ring connections give reason to speculate that FC effects follow the reduced structural integrity of the brain network and arise not before the damage to white matter pathways has reached a certain extent. These findings are also in line with the observation in other neurodegenerative diseases that significant structural loss has occurred before clinical signs or dysfunctioning manifest [Dickerson and Wolk, 2012; Wu et al., 2011]. The correlation between disability (i.e., ALSFRS-R scores) and first ring SC changes and the absence of correlations between FC changes and disability might be another indication that structural damage has more clinical significance. Our results suggest that, of the measures explored here, first ring SC changes may hold potential as a biomarker. A longitudinal study comparing the spread of SC impairment to that of FC impairment at different time points may help to further unravel the relation between SC and FC changes. In case reduced SC is followed by impaired FC, a functional parallel of the expanding loss of motor network structure [Verstraete et al., 2013] might be observed at later stages of the disease.

One of the limitations of our study is that only direct functional connections were included for analysis. As the aim of this study was to determine the relation between SC and FC impairments, it seems justified to just include direct connections so that a change in SC and FC could be computed for every connection. In addition, in our study a group threshold of 50% was chosen. A *post hoc* analysis in which results were examined for thresholds ranging from 30 to 70% [de Reus and

van den Heuvel, 2013], did not change the nature of our findings, implying the analyses are robust against group threshold selection. Another methodological consideration is that in diffusion tensor imaging (DTI) diffusion profiles are fitted a

TABLE III. Ring classification of cortical and sub-cortical nodes surrounding the right motor cortex

| First ring nodes	Second ring nodes
Inferior parietal	Medial orbitofrontal
Superior frontal	Rostral anterior cingulate
Postcentral	Posterior cingulated
Superior parietal	Caudal anterior cingulate
Pallidum[a]	Frontal pole
Brain stem[a]	Lateral occipital
Hippocampus[a]	Fusiform
Thalamus proper[a]	Pericalcarine
Caudal middle frontal	Cuneus
Putamen[a]	Precuneus
Insula	Isthmus cingulated
Superior temporal	Lingual
Parsopercularis	Caudate[a]
Supramarginal	Entorhinal
	Parahippocampal
	Amygdala[a]
	Inferior temporal
	Accumbens area[a]
	Temporal pole
	Rostral middle frontal
	Lateral orbitofrontal
	Parsorbitalis
	Parstriangularis
	Transverse temporal
	Posterior banks of superior temporal
	Middle temporal

[a]Subcortical brain region.
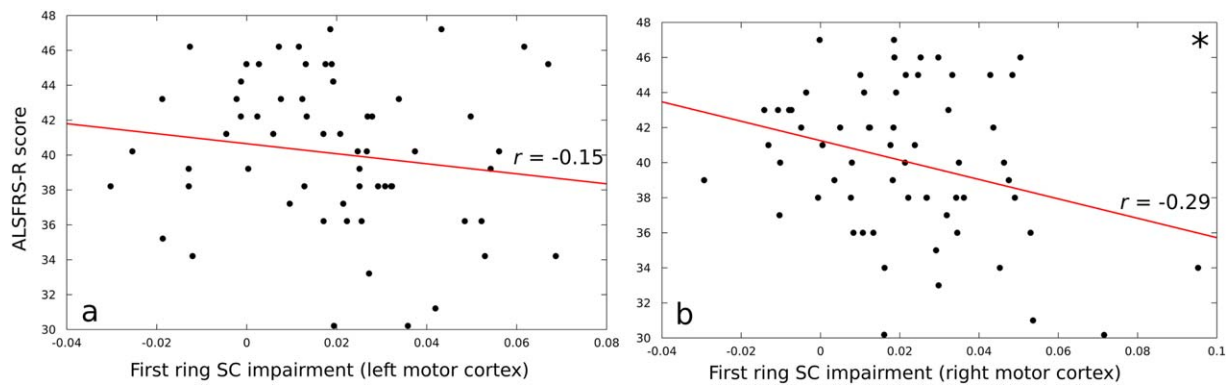
Figure 6.

Scatter plot of ALSFRS-R scores versus first ring SC impairments of the left (**a**) and right (**b**) motor cortices. (*) denotes statistical significance of the correlation ($P = 0.02$). [Color figure can be viewed in the online issue, which is available at wileyonlinelibrary.com.]

single tensor, which cannot describe a diffusion profile corresponding to crossing fibers and is known to yield inaccurate FA values in such voxels [Johansen-Berg and Rushworth, 2009; Jbabdi and Johansen-berg, 2011; Pullens et al., 2010]. As a result, SC effects, notably in white matter tracts between frontal and posterior regions crossing each other at the level of the corona radiata, may not be picked up. While alternative methods, such as probabilistic or multitensor approaches, may better detect these fibers, deterministic fiber tracking measuring connection strengths instead of probabilities, is more appropriate for the use of weighted networks. Therefore, for the type of analyses performed in the current study, DTI fiber tracking was the preferred method. Furthermore, findings of FC effects should be carefully assessed in light of the significant between-subject variation in rs-fMRI connectivity data [Chou, 2012]. Future studies based on larger cohorts of patients and healthy controls, e.g., the combined effort of the Neuroimaging Symposium in ALS (NISALS) collaborators [Turner et al., 2011], will have to confirm the FC effects brought forward in this study.

CONCLUSION

The present findings demonstrate a clear link between changes in SC and FC in ALS, suggesting the pathogenic process affects both structural and FC of the brain. The observed coupling between SC and FC effects provides reason to explore possible causality. A better understanding of the structure-function relation may provide new insights that direct the focus in biomarker development towards structural or functional measures.

ACKNOWLEDGMENTS

Figure 7.

Scatter plot of changes in FA and FC in patients averaged over each node's direct connections fitted by a line with a positive gradient, indicating a positive correlation between changes in FA and FC. Positive connectivity changes denote impairments and negative connectivity changes mark enhancements. The color scheme to distinguish between motor cortex, first ring and second ring nodes (Table III) corresponds with that of Figure 4. [Color figure can be viewed in the online issue, which is available at wileyonlinelibrary.com.]

REFERENCES

Agosta F, Valsasina P, Absinta M, Riva N, Sala S, Prelle A, Copetti M, Comola M, Comi G, Filippi M (2011): Sensorimotor functional connectivity changes in amyotrophic lateral sclerosis. Cereb Cortex 21:2291–2298.
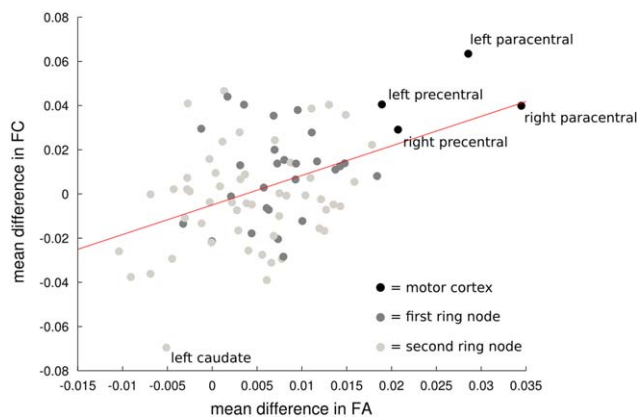
Alstott J, Breakspear M, Hagmann P, Cammoun L, Sporns O (2009): Modeling the impact of lesions in the human brain. PLoS Comput Biol 5:e1000408.

Brooks BR, Miller RG, Swash M, Munsat TL (2000): El Escorial revisited: Revised criteria for the diagnosis of amyotrophic lateral sclerosis. Amyotroph Lateral Scler Other Motor Neuron Disord 1:293–299.

Chai XJ, Castañón AN, Ongür D, Whitfield-Gabrieli S (2012): Anti-correlations in resting state networks without global signal regression. NeuroImage 59:1420–1428.

Chang L-C, Jones DK, Pierpaoli C (2005): RESTORE: Robust estimation of tensors by outlier rejection. Magn Reson Imaging 53:1088–1095.

Chou Y (2012): Investigation of long-term reproducibility of intrinsic connectivity network mapping: A resting-state fMRI study. AJNR. Am J Neuroradiol 33:833–838.

Cirillo M, Esposito F, Tedeschi G, Caiazzo G, Sagnelli A, Piccirillo G, Confroti R, Tortora F, Monsurro M, Cirillo S, Trojsi F (2012): Involvement in amyotrophic lateral sclerosis: A whole-brain DTI study. AJNR. Am J Neuroradiol 33:1102–1108.

Collin G, Sporns O, Mandl RCW, van den Heuvel MP: Structural and functional aspects relating to cost and benefit of rich club organization in the human cerebral cortex. Cereb Cortex doi: 10.1093/cercor/bht064. [Epub ahead of print]

Cordes D, Haughton VM, Arfanakis K, Carew JD, Turski PA, Moritz CH, Quiqley MA, Meyerand ME (2001): Frequencies contributing to functional connectivity in the cerebral cortex in "resting-state" data. AJNR Am J Neuroradiol 22:1326–1333.

de Reus MA, van den Heuvel MP (2013): Estimating false positives and negatives in brain networks. NeuroImage 70:402–409.

del Aguila MA, Longstreth WT, McGuire V, Koepsell TD, van Belle G (2003): Prognosis in amyotrophic lateral sclerosis: A population-based study. Neurology 60:813–819.

Dickerson BC, Wolk DA (2012): MRI cortical thickness biomarker predicts AD-like CSF and cognitive decline in normal adults. Neurology 76:84–90.

Douaud G, Filippini N, Knight S, Talbot K, Turner MR (2011): Integration of structural and functional magnetic resonance imaging in amyotrophic lateral sclerosis. Brain 134:3470–3479.

Fischl B, van der Kouwe A, Destrieux C, Halgren E, Ségonne F, Salat DH, Busa E, Seidman LJ, Goldstein J, Kennedy D, Caviness V, Makris N, Rosen B, Dale AM (2004): Automatically parcellating the human cerebral cortex. Cereb Cortex 14:11–22.

Fischl B, Sereno MI, Dale AM. (1999): Cortical surface-based analysis. NeuroImage 9:195–207.

Fox MD, Snyder AZ, Vincent JL, Corbetta M, Van Essen DC, Raichle ME (2005): The human brain is intrinsically organized into dynamic, anticorrelated functional networks. Proc Natl Acad Sci U S A 102:9673–9678.

Hagmann P, Cammoun L, Gigandet X, Meuli R, Honey CJ, Wedeen VJ, Sporns O (2008): Mapping the structural core of human cerebral cortex. PLoS Biol 6:e159.

Hardiman O, van den Berg LH, Kiernan MC (2011): Clinical diagnosis and management of amyotrophic lateral sclerosis. Nat Rev Neurol 7:639–649.

Jbabdi S, Johansen-berg H. (2011): Tractography—where do we go from here? Brain Connect 1:169–183.

Johansen-Berg H, Rushworth MFS. (2009): Using diffusion imaging to study human connectional anatomy. Annu Rev Neurosci 32:75–94.

Mohammadi B, Kollewe K, Samii A, Krampfl K, Dengler R, Münte TF (2009): Changes of resting state brain networks in amyotrophic lateral sclerosis. Exp Neurol 217:147–153.

Mori S, van Zijl PCM (2002): Fiber tracking: principles and strategies—A technical review. NMR Biomed 15:468–480.

Mori S, Crain BJ, Chacko VP, van Zijl PC (1999): Three-dimensional tracking of axonal projections in the brain by magnetic resonance imaging. Ann Neurol 45:265–269.

Mori S, Kaufmann WE, Davatzikos C, Stieltjes B, Amodei L, Fredericksen K, et al. (2002): Imaging cortical association tracts in the human brain using diffusion-tensor-based axonal tracking. Magn Reson Med 47:215–223.

Prudlo J, Bißbort C, Glass A, Grossmann A, Hauenstein K, Benecke R, et al. (2012): White matter pathology in ALS and lower motor neuron ALS variants: A diffusion tensor imaging study using tract-based spatial statistics. J Neurol 259:1848–1859.

Pullens P, Roebroeck A, Goebel R. (2010): Ground truth hardware phantoms for validation of diffusion-weighted MRI applications. J Magn Reson Imaging 32:482–488.

Rose S, Pannek K, Bell C, Baumann F, Hutchinson N, Coulthard A, McCombe P, Henderson R (2012): Direct evidence of intra- and interhemispheric corticomotor network degeneration in amyotrophic lateral sclerosis: An automated MRI structural connectivity study. NeuroImage 59:2661–2669.

Seeley WW, Crawford RK, Zhou J, Miller BL, Michael D (2009): Neurodegenerative diseases target large-scale human brain networks. Neuron 62:42–52.

Sporns O (2006): Small-world connectivity, motif composition, and complexity of fractal neuronal connections. Biosystems 85:55–64.

Stam CJ, Reijneveld JC (2007): Graph theoretical analysis of complex networks in the brain. Nonlinear Biomed Phys 1:3.

Turner MR, Grosskreutz J, Kassubek J, Abrahams S, Agosta F, Benatar M, Filippi M, Goldstein LH, van den Heuvel M, Kalra S, Lule D, Mohammadi B, first Neuroimaging Symposium in ALS (NISALS) (2011): Towards a neuroimaging biomarker for amyotrophic lateral sclerosis. Lancet Neurol 10:400–403.

van den Heuvel MP, Hulshoff Pol HE (2010): Exploring the brain network: A review on resting-state fMRI functional connectivity. Eur Neuropsychopharmacol 20:519–534.

van den Heuvel MP, Sporns O. (2011): Rich-club organization of the human connectome. J Neurosci 31:15775–15786.

van den Heuvel MP, Sporns O, Collin G, Scheewe T, Mandl RCW, Cahn W, et al. (2013): Abnormal rich club organization and functional brain dynamics in schizophrenia. JAMA Psychiatry 70:783–792.

Verstraete E, van den Heuvel MP, Veldink JH, Blanken N, Mandl RC, Hulshoff Pol HE, van den Berg LH (2010): Motor network degeneration in amyotrophic lateral sclerosis: A structural and functional connectivity study. PloS One 5:e13664.

Verstraete E, Veldink JH, Mandl RCW, van den Berg LH, van den Heuvel MP (2011): Impaired structural motor connectome in amyotrophic lateral sclerosis. PloS One 6:e24239.

Verstraete E, Veldink JH, van den Berg LH, van den Heuvel MP: Structural brain network imaging shows expanding disconnection of the motor system in amyotrophic lateral sclerosis. Hum Brain Mapp doi: 10.1002/hbm.22258. [Epub ahead of print]

Wu Y, Le W, Jankovic J (2011): Preclinical biomarkers of Parkinson disease. Arch Neurol 68:22–30.

Zalesky A, Fornito A, Bullmore ET (2010): Network-based statistic: Identifying differences in brain networks. NeuroImage 53: 1197–1207.

Zhou F, Gong H, Li F, Zhuang Y, Zang Y, Xu R, Wang Z (2013): Altered motor network functional connectivity in amyotrophic lateral sclerosis: a resting-state functional magnetic resonance imaging study. Neuroreport 24:657–662.